fire

MDPI

Article

Characteristics of Carbon Monoxide and Ethylene Generation in Mine's Closed Fire Zone and Their Influence on Methane Explosion Limits

Dong Ma [1], Leilin Zhang [2,*], Tingfeng Zhu [3] and Zhenfang Shi [3]

[1] State Key Laboratory for Fine Exploration and Intelligent Development of Coal Resources, China University of Mining and Technology, Xuzhou 221008, China
[2] Engineering Technology Research Centre for Safe and Efficient Coal Mining, Anhui University of Science and Technology, Huainan 232001, China
[3] School of Safety Engineering, China University of Mining and Technology, Xuzhou 221116, China
* Correspondence: 2014017@aust.edu.cn

Abstract: Methane explosions often occur during the closure process of mine fire zones, during which the concentration of combustible gases such as monoxide and ethylene produced by coal combustion dynamically changes, which changes the risk of methane explosion. Therefore, studying the gas concentration distribution and methane explosion limits during the process of mine closure is of great significance for disaster prevention and control. In this paper, a three-dimensional physical model of gob was built, and the distribution of monoxide and ethylene in the process of fire zone closure was investigated. Further, the explosion limits of methane enriched with CO and C_2H_4 in the closed fire zone of gob were analyzed. The results indicate that CO and C_2H_4 would form a small-scale accumulation phenomenon near the fire zone after the closure of the fire zone, and when the fire zone is closed for more than 15 min, the mixed combustible gases in the environment lose their explosiveness.

Keywords: coal mine fires; methane explosion; closed fire zone; explosion limit

Citation: Ma, D.; Zhang, L.; Zhu, T.; Shi, Z. Characteristics of Carbon Monoxide and Ethylene Generation in Mine's Closed Fire Zone and Their Influence on Methane Explosion Limits. *Fire* **2024**, *7*, 168. https://doi.org/10.3390/fire7050168

Academic Editors: Chuyuan Huang, Haipeng Jiang and Lijuan Liu

Received: 13 March 2024
Revised: 11 May 2024
Accepted: 12 May 2024
Published: 14 May 2024

1. Introduction

Mine fires have always been a major safety hazard, causing significant casualties and economic losses [1–3]. In order to prevent the expansion of a mine fire and control the disaster, the timely closure of the affected zone is an important emergency measure [4–6]. After the sealing, the oxygen supply to the fire zone is cut off from outside, so the heat generated inside the fire zone is less than the heat dissipated, which reduces the internal temperature of the fire zone and effectively controls the development of the fire [7–9]. Furthermore, once the fire zone is sealed, the oxygen concentration also decreases so the coal enters a negative combustion state. This generates a significant amount of flammable gases, including CO and C_2H_4. These gases accumulate in the closed fire zone, making it susceptible to methane explosions [10]. For instance, the Jilin Babao mine experienced a massive methane explosion during the closure process in 2013, resulting in the tragic death of 53 workers [11]. Similarly, a methane explosion in the Soma mine in Turkey caused the death of 301 workers in 2014 due to improper operation of a closed fire zone [12].

To better understand the internal gases' composition and combustion state after the fire zone is sealed, the indicator gases in the process of fire zone sealing are often used for risk prediction and assessment. Carbon monoxide and ethylene, as predictors of coal combustion, are the main combustible gases produced in the process of coal combustion [13]. Understanding the coal's combustion state is crucial for comprehending the mechanism of explosive accidents during hole sealing and preventing future incidents.

In practice, it is difficult to study the gas distribution in the fire zone using on-site measurements. Therefore, researchers tend to use numerical simulation and experimental

platform methods for their study. Zhu et al. [14] used numerical simulation to study the effect of N_2 injection in a sealed fire zone on the development of a fire and found the transport law of the gas mixture in the fire zone. Wang et al. [15] used numerical simulation to study the distribution pattern of CH_4 and smoke after the fire zone was closed, as well as the influencing factors of the methane explosion's range. It was found that fire smoke will affect the methane explosion range, and the explosion zone first appeared in the return air side. Brune and Saki [16] used a computational fluid dynamics model to study the dynamic sealing of a progressive sealed longwall gob with nitrogen. They found that this approach can separate methane and air, thereby reducing the risk of explosion. However, although numerical simulation can solve some of the research problems, the use of numerical simulation for complex mine environments, where parameters such as coal-rock porosity and oxygen consumption are often assumed, can lead to unavoidable errors in the experimental results. Therefore, building a physical experimental platform is the most appropriate method for studying the distribution of flue gas before and after the sealing. Zhou et al. [5] used an experimental platform to study the gas changes in the fire zone after opening and found an instantaneous elevation of CO after the rekindling of the opening. Wen et al. [17] used a homemade high-temperature coal spontaneous combustion experimental setup to study the great influence of oxygen on coal spontaneous combustion at different temperatures in the sealed fire zone. Shi et al. [6] studied the impact of sealed fire zones on methane explosions and found that sealing could lead to changes in temperature and CH_4 concentration, as well as cause methane migration, which can concentrate in the fire zone. Zheng et al. [18] used a physical model to study the coupling effect of gas and temperature in the mining airspace and concluded that the temperature of the airspace leakage area should be monitored to prevent causing methane explosion accidents. Wang et al. [19] studied the effects of different sealing methods on the generation and flow of smoke in fire zones by building gob models and found that sealing methods had a great impact on the development of fires, which may lead to methane explosion accidents.

So far, much research has been carried out regarding the closed fire zone, but there is a lack of research related to CO and C_2H_4 in the process of fire zone closure. Therefore, in this paper, an experimental platform for the modeling of the mining zone was established, and the change law of the distribution of the indicator gases in the process of fire zone closure was investigated. In the study, the dynamics of CO and C_2H_4 transport and distribution were delineated during the thermal escalation of coal under conditions of spontaneous combustion. Further, the explosion limits of methane enriched with CO and C_2H_4 mixtures were tested. From the insights gleaned, the distribution pattern of CO and C_2H_4 gases at different temperatures in the closed fire zone were conducive to predicting the combustion state of enclosed fire zones.

2. Materials and Methods

2.1. Gob Platform

To investigate the gas concentration changes during spontaneous coal combustion and closure in the mining zone, a three-dimensional physical model of gob was constructed, as shown in Figure 1. The schematic diagram of the physical model is shown in Figure 2. The experimental platform comprises the gob, the working face, the intake and return air roadways, the coal combustion chamber, the ventilation system, the temperature monitoring system and the gas collection and analysis system. This ventilation system is a variable-frequency mixed-flow duct fan, as the fan supplies air to the working face. Additionally, the ventilator was connected to the working face by an air duct, and a hot-wire anemometer measures the internal ventilation of the working face before each test. The temperature monitoring system was made up of a heating plate, a temperature controller, a temperature sensor and a data acquisition card. Considering the temperature control and monitoring of the fire source in the spontaneous combustion zone of coal, the heat source of the experiment is the coal powder heated by the heating plate. Thermocouples were used to connect to the TES1310 pyrometer (Furuida Instrument Technology Co., Ltd.,

Dongguan, China) for real-time monitoring of the internal temperature of the coal. As a result, the experiment focuses on the internal temperature and concentration fields of the gob. Therefore, through the gas sample collection and analysis system, the simulated internal flue gas component and the concentration distribution law of the air mining zone can be quantitatively derived. Table 1 displays the specific dimensions of the gob.

Figure 1. Experimental platform.

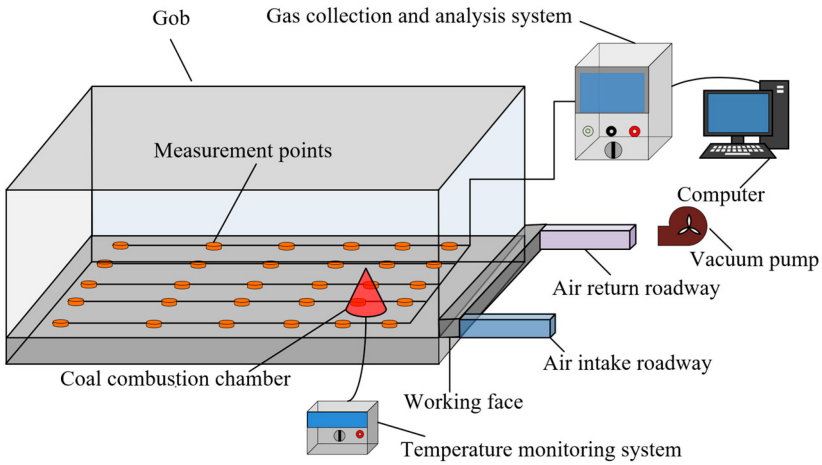

Figure 2. Schematic diagram of the three-dimensional physical model of gob.

Table 1. The dimensions of the gob.

Part	Length/cm	Width/cm	Height/cm
Mining face	120	5	3
Air intake roadway	20	4	3
Air return roadway	20	4	3
Mine gob	180	120	80

2.2. Methods

The experimental platform is set up with a layer of measurement points, with the distance from the measurement points to the ground being 1 cm. The layer of measurement points is arranged in 5 rows along the strike direction of the gob and 5 columns along the inclination direction, a total of 25 measurement points. As shown in Figure 3, the focus of

this study is the area near the combustion chamber of the coal, which includes a total of 9 measurement points. The analysis and research mainly rely on the experimental data from the monitoring points on two monitoring lines, L1 and L2. Prior to each experiment, the ventilation velocity was measured with a hot wire anemometer to ensure that the wind speed conditions of the working face reached 0.6 m/s. At the inception of the experiment, 100 g of coal powder was placed on the heating plate with the highest temperature of 400 °C, and the thermocouple was embedded in the coal. The thermocouple was connected to the TES1310 temperature tester to monitor the temperature of the coal. Subsequently, an automatic negative-pressure gas sampler was used to collect gas generated during the fire zone closure process. Finally, a gas chromatograph was used to detect the composition of the flue gas to obtain its distribution and concentration at different temperatures and different positions. There were 4 aspects of uncertainty in the experiment: deviation of gas concentration during gas distribution (A1), error arising during pumping tests (A2), error in ventilation velocity at the working face (A3) and error from ambient temperature (A4). The deviation of the gas concentration during gas distribution (A1) and the error arising during the pumping test (A2) originate from the accuracy of the instrument, with an error of about 0.3%. The error in the ventilation velocity at the working face (A3) and the error from ambient temperature (A4) come from the testing instruments and manual readings, with an error of about 3.2%. Thus, the total experimental uncertainty $\sqrt{A1^2 + A2^2 + A3^2 + A4^2}$ is less than 5%.

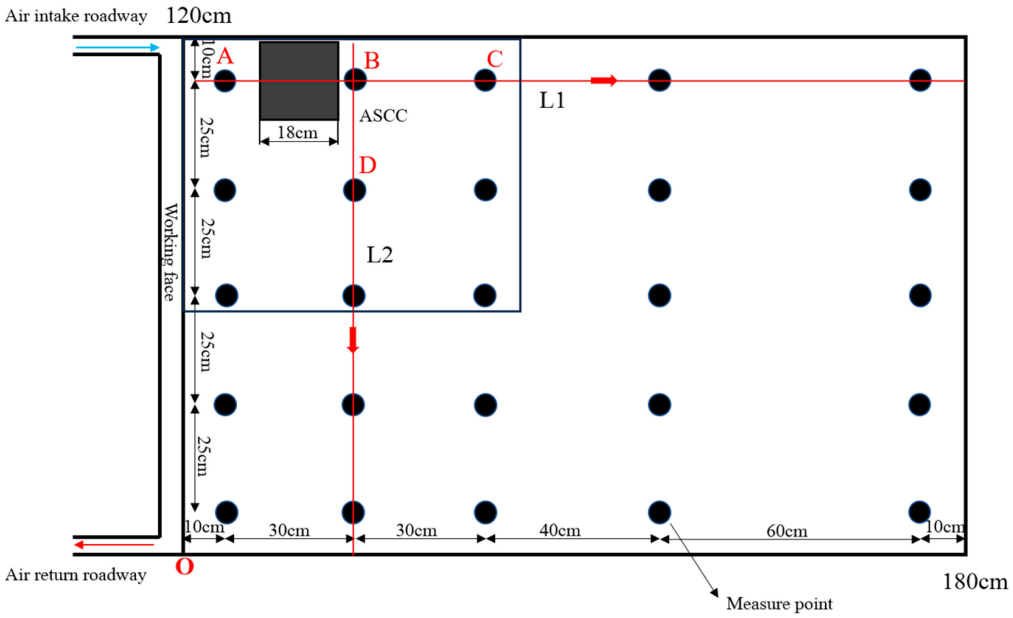

Figure 3. Layout of model measuring points.

3. Results and Discussion

3.1. The Distribution of CO in the Closed Fire Zone of Gob

As discernible from Figure 4, when the fire zone was not sealed, the combustion intensified with the rise in coal temperature, leading to substantial production of CO and a sharp increase in its concentration. As shown in Figure 4a, when the temperature increased to 100 °C, a portion of the CO was discharged along the working face into the air return roadway. Additionally, due to the presence of gob leakage, another portion of CO flowed towards the deeper and upper parts of the gob. When the coal temperature reached 250 °C, the area of high CO concentration moved further away from the working face, as shown in Figure 4b. Moreover, owing to the gas vortex phenomenon in coal spontaneous combustion fire zone, it resulted in a much higher CO concentration at the accumulation than in the surrounding area [20]. Since then, the fire zone was sealed. It can be seen from Figure 4 that the temperature in the fire zone showed a trend of increasing and then decreasing.

When the coal temperature reached 400 °C, the CO concentration increased dramatically, and its distribution area moved further into the deeper part of the gob. During the cooling process, due to the absence of intake airflow, the coal spontaneous combustion flue gas was only influenced by the thermal buoyancy movement of the gas, and the influence range was smaller than the heating process. As shown in Figure 4d, when the coal temperature was reduced to 300 °C, the area of high concentration of CO was mainly near the high-temperature point, deep in the gob, and near the air return roadway. As shown in Figure 4e, when the temperature was lowered to 250 °C, the region of high CO concentration was mainly near the high temperature point, and the distribution of CO was further balanced. When the temperature was further reduced, the distribution of CO was more balanced and basically distributed in all locations of the gob, as shown in Figure 4f.

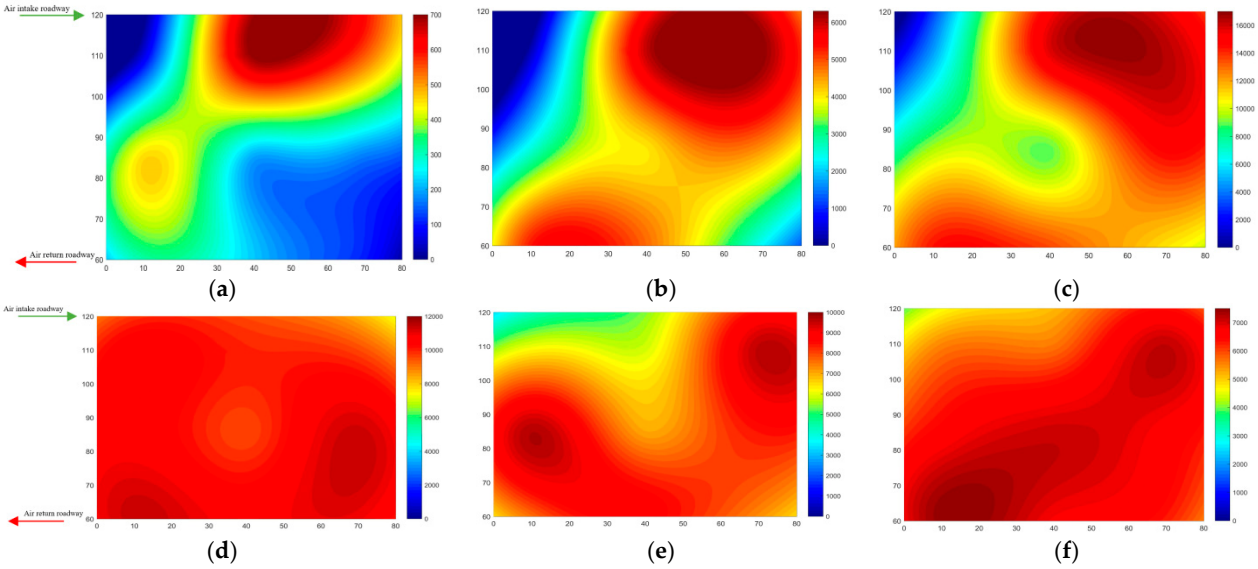

Figure 4. CO concentration under different coal temperature conditions. (**a**) Coal temperature 100 °C; (**b**) coal temperature 250 °C; (**c**) coal temperature 400 °C; (**d**) coal temperature 300 °C; (**e**) coal temperature 250 °C; (**f**) coal temperature 100 °C.

The variation of CO concentration on the two monitoring lines, L1 and L2, are shown in Figures 5 and 6. During the temperature rise and fall periods, the CO concentration at different temperatures shows an initially increasing and then decreasing strike direction of the gob. However, the inclination direction of the gob showed fluctuating changes. As shown in Figure 5a, when the coal temperature was 250 °C, the CO concentrations of the measuring points on the monitoring line L1 were 32 ppm, 4246 ppm, 6355 ppm, 3500 ppm and 100 ppm, respectively, and the highest concentration was near the middle of the strike direction of the gob. As shown in Figure 6a, when the coal temperature was 400 °C, the CO concentrations of the measuring points on the monitoring line L2 were 800 ppm, 3000 ppm, 14,386 ppm, 9435 ppm and 13,127 ppm, respectively, and the highest concentration was near the middle of the inclination direction of the gob. The CO concentrations in the strike direction and the inclination direction showed an increase with coal temperature increase. For example, as shown in Figure 5a, the CO concentrations at measurement point B were 542 ppm, 4246 ppm and 13,127 ppm at coal temperatures of 100 °C, 250 °C and 400 °C, respectively.

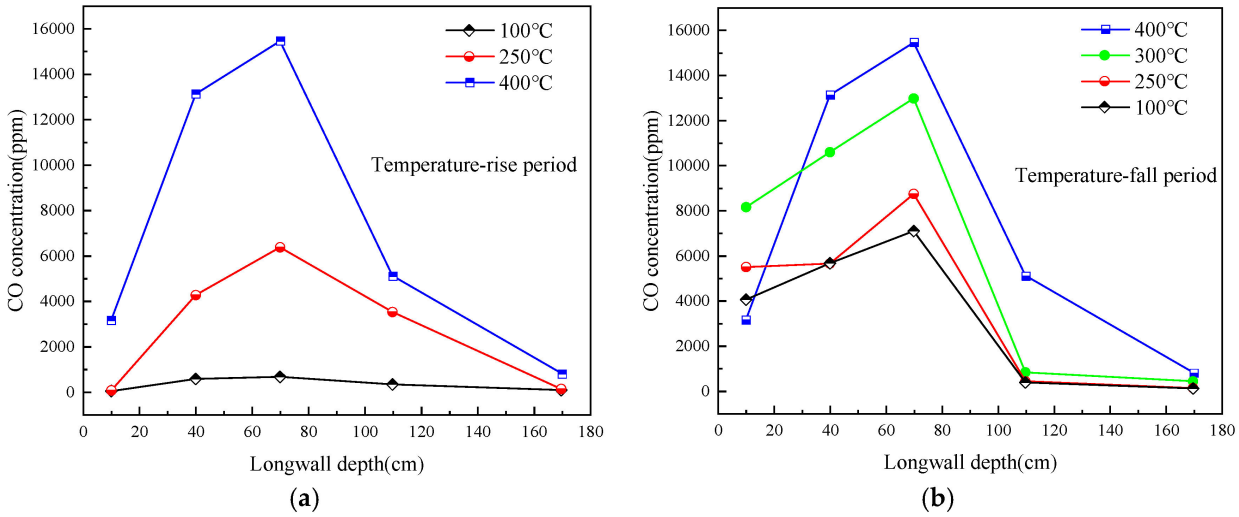

Figure 5. Changes in CO concentration at different temperatures in the L1 monitoring line. (**a**) Temperature-rise period; (**b**) temperature-fall period.

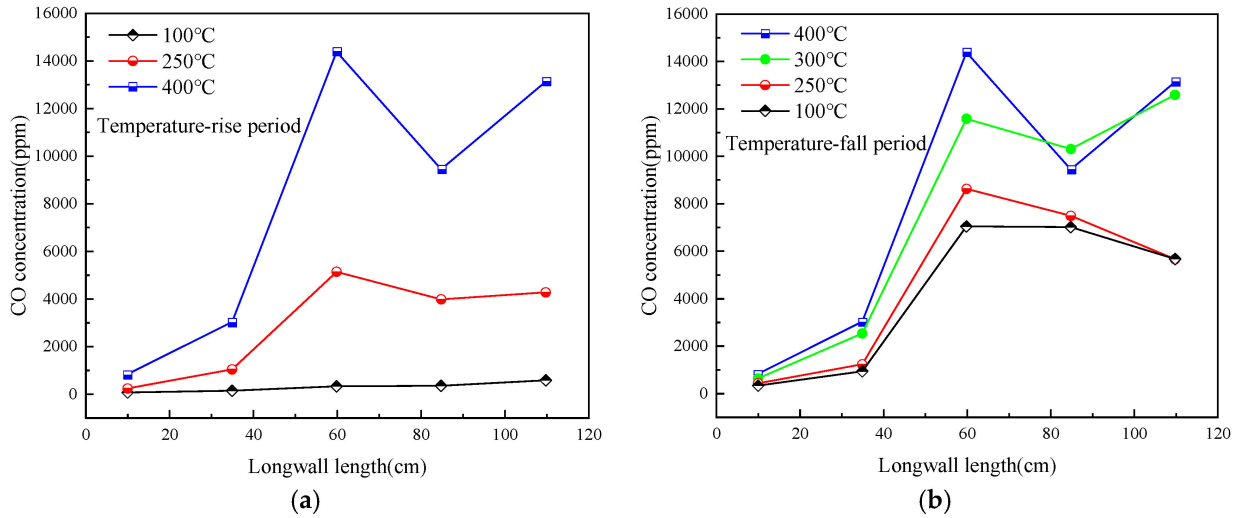

Figure 6. Changes in CO concentration at different temperatures in the L2 monitoring line. (**a**) Temperature-rise period; (**b**) temperature-fall period.

3.2. The Distribution of C_2H_4 in the Closed Fire Zone of Gob

Figure 7 shows the distribution of C_2H_4 concentration. As can be seen in Figure 7a, when the coal temperature reached up to 100 °C, the C_2H_4 concentration generated by the combustion of the coal was relatively small. Although it was influenced by the intake airflow, most of the deep part of the gob was not detected in a higher concentration of C_2H_4, with an average concentration of less than 10 ppm. With the increase in the temperature of the coal, there is a significant rise in the concentration of C_2H_4 generated in the inner part of the gob. As the temperature of the coal reached up to 250 °C, as shown in Figure 7b, there was a small accumulation of C_2H_4 concentration near the high-temperature point, and the maximum concentration was less than 150 ppm. Subsequently, as the fire zone was closed, as shown in Figure 7c, the concentration of C_2H_4 continued to increase, which gradually spread to the deep part of the gob and the air return side under the influence of the intake airflow. Due to the closure of the fire zone, resulting in a gradual decrease in the temperature of the gob, C_2H_4 concentration generation was reduced and uniformly distributed in the deep part of the gob, the coal temperature dropped to 300 °C and the C_2H_4 concentration of the various measurement points was between 50 and 60 ppm,

as shown in Figure 7d. However, when the coal temperature dropped to 250 °C, as in Figure 7e, the C_2H_4 concentration on the intake side appeared to drop roughly 20 ppm. Additionally, the air return side and the deep part of the gob still showed a wide range of C_2H_4 accumulation. Finally, when the coal temperature reached up to 100 °C, the C_2H_4 concentration showed a significant decrease, and the maximum concentration did not exceed 50 ppm.

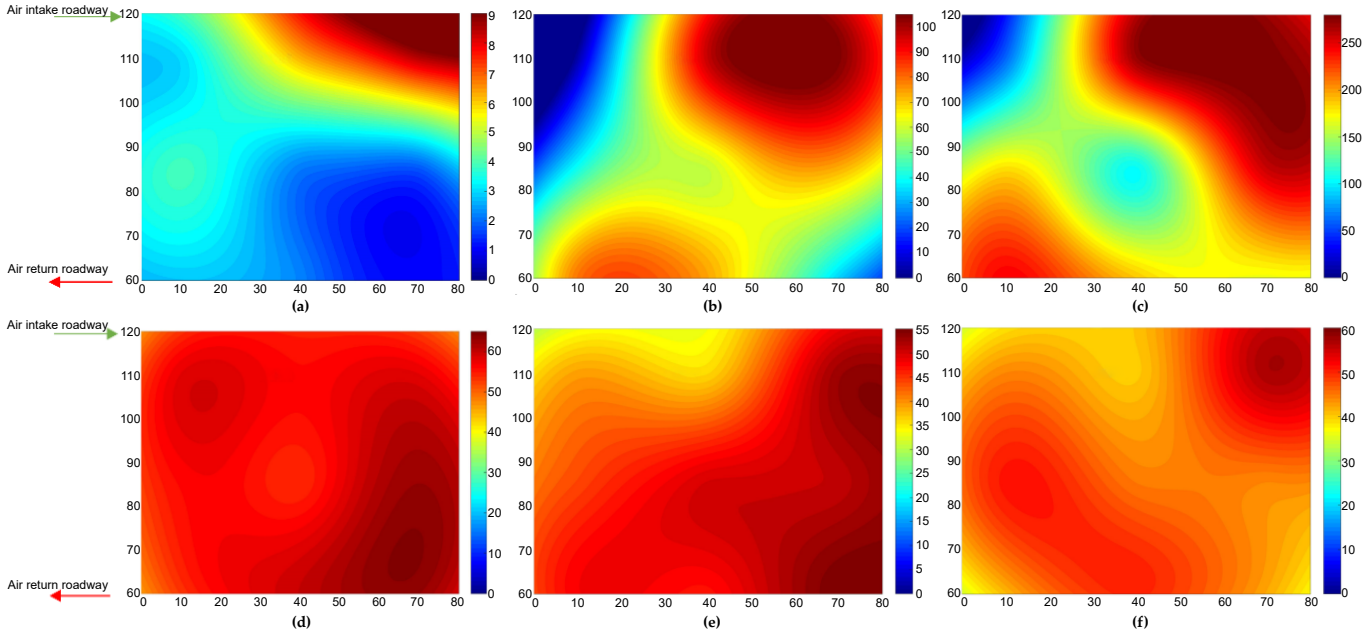

Figure 7. C_2H_4 concentration under different coal temperature conditions. (**a**) Coal temperature 100 °C; (**b**) coal temperature 250 °C; (**c**) coal temperature 400 °C; (**d**) coal temperature 300 °C; (**e**) coal temperature 250 °C; (**f**) coal temperature 100 °C.

The changes in C_2H_4 concentration along the two monitoring lines, L1 and L2, are shown in Figures 8 and 9. As can be seen from Figure 8a, along the direction of the monitoring line L1, C_2H_4 shows a trend of increasing and then decreased under different temperature conditions. For example, when the coal temperature was 250 °C, the C_2H_4 concentration increased from 9 ppm to 110 ppm and then decreased to 20 ppm. When the coal temperature was 400 °C, the C_2H_4 increased from 30 ppm to 260 ppm and then decreased to 5 ppm. After the closure of fire zone, as shown in Figure 8b, the C_2H_4 concentration was basically the same as that in the temperature-rise period. As the temperature decreased to 300 °C, the C_2H_4 concentration increased from 52 ppm by 5 ppm and then decreased to 8 ppm. Comparing the C_2H_4 concentration at different temperatures, it can be seen that there was a good linear relationship between the coal temperature and the C_2H_4 concentration. Moreover, as shown in Figure 9b, when the temperature of the coal decreased to 300 °C, the concentration of C_2H_4 increased from 4 ppm to 59 ppm and then decreased to 55 ppm. Overall, the C_2H_4 concentration decreased with the coal temperature decreases in the temperature-fall period, and the peak C_2H_4 concentration ranged from 110 ppm to 50 ppm from 400 °C to 100 °C.

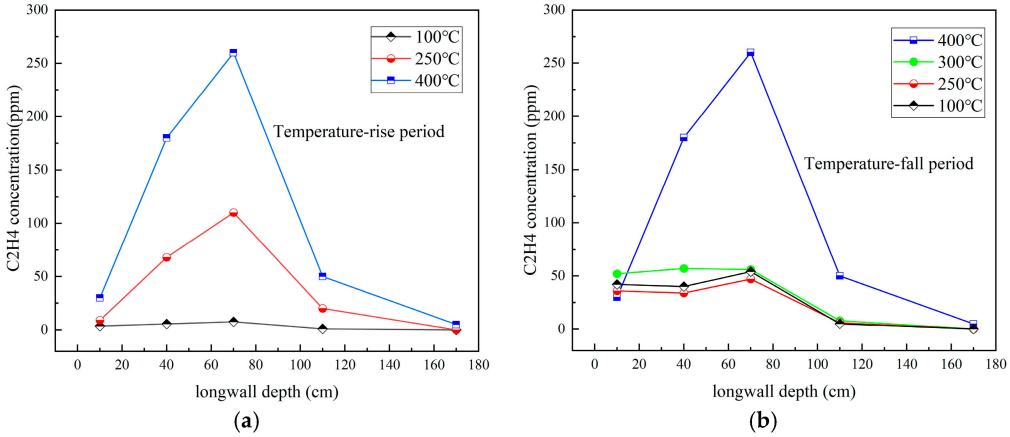

Figure 8. Changes in C_2H_4 concentration in the L1 monitoring line. (**a**) Temperature-rise period; (**b**) temperature-fall period.

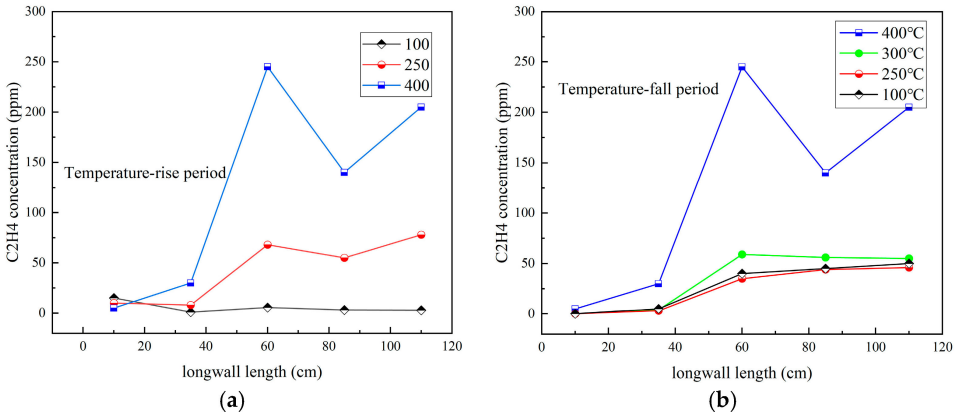

Figure 9. Changes in C_2H_4 concentration in the L2 monitoring line. (**a**) Temperature-rise period; (**b**) temperature-fall period.

3.3. The Methane Explosion Concentration in the Closed Fire Zone of Gob

Combustible mixed gases mixed with oxygen may explode if they encounter a sufficiently high-energy ignition source. When the concentration of air or oxygen is high enough, the concentration of combustible mixed gases is low and causes a lean combustion state, and there is not enough fuel to maintain the explosion reaction. On the contrary, if the concentration of combustibles is high and the concentration of air or oxygen is low, the combustibles are in a lean oxygen state, and there is not enough oxygen to assist the explosion reaction. Combustible mixed gases must be within the range of the lower explosive limit and upper explosive limit in order to explode.

The testing of methane explosion limits is based on a 20 L spherical explosion system, as introduced in reference [21]. The system mainly includes a 20 L approximately spherical explosive reaction vessel, ignition device, gas distribution system, vacuum pumping system, data acquisition system, controller, high-speed camera. The inner diameter of a 20 L approximately spherical explosion reaction vessel was about 34 cm, and the maximum pressure of the reaction vessel can reach 4 MPa, which can ensure the safe conduct of mixed gas explosion experiments. The ignition device consists of an ignition electrode located at the center of a spherical reaction vessel and an external electric spark generator. After the gas balance in the reactor, the ignition device was automatically controlled by a controller. In the experiment, the ignition energy was 60 J, and the ignition delay time was 120 ms. The gas distribution system mainly consisted of gas cylinders, air compressors, flow meters and vacuum pumps. The gas cylinders used in the experiment were 99.99% pure CH_4, CO, C_2H_4, O_2 and N_2 cylinders. The mixed gas was configured using the partial pressure method, and the gas distribution

accuracy was 0.1%. During the experiment, the ambient temperature was 18 °C~25 °C, the air humidity was 55%~65% and the pressure was 0.1 MPa.

According to the EU BSEN 1839:2012 standard [22], this paper takes whether the maximum explosion pressure exceeded (5 ± 0.1)% of the initial pressure as the standard for explosion occurrence. Each operating condition experiment should be repeated at least three times to ensure good accuracy and repeatability of the test results.

The oxygen concentration changes at four monitoring points near the fire area are shown in Figure 10. It can be seen that after the fire zone is closed, the oxygen concentration at the measuring points showed a rapid decreasing trend and eventually approached complete depletion. Among them, the oxygen concentration at point B decreased the fastest. When the fire zone was closed for 20 min, the oxygen concentration at point B was consumed to nearly 0%, while points A, C and D decreased to nearly 0% after 22 min, 25 min and 26 min, respectively. Based on the O_2 concentration, CO concentration and C_2H_4 concentration of these four measurement points, the methane explosion limit of the monitoring points during the fire zone closure process were tested, as shown in Figure 11.

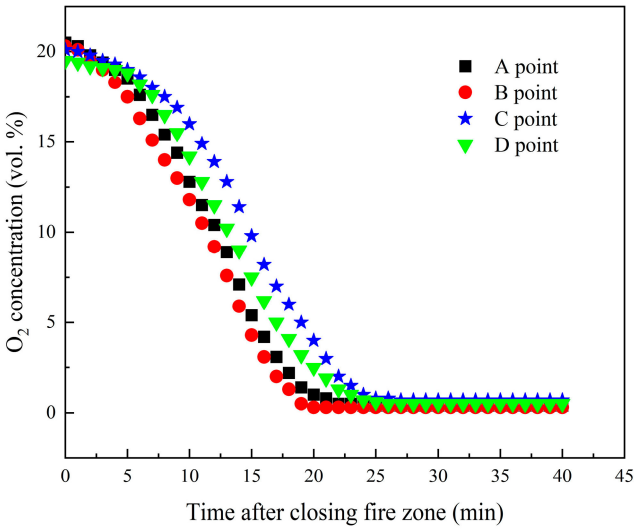

Figure 10. The variation of O_2 concentration in the zone near the fire.

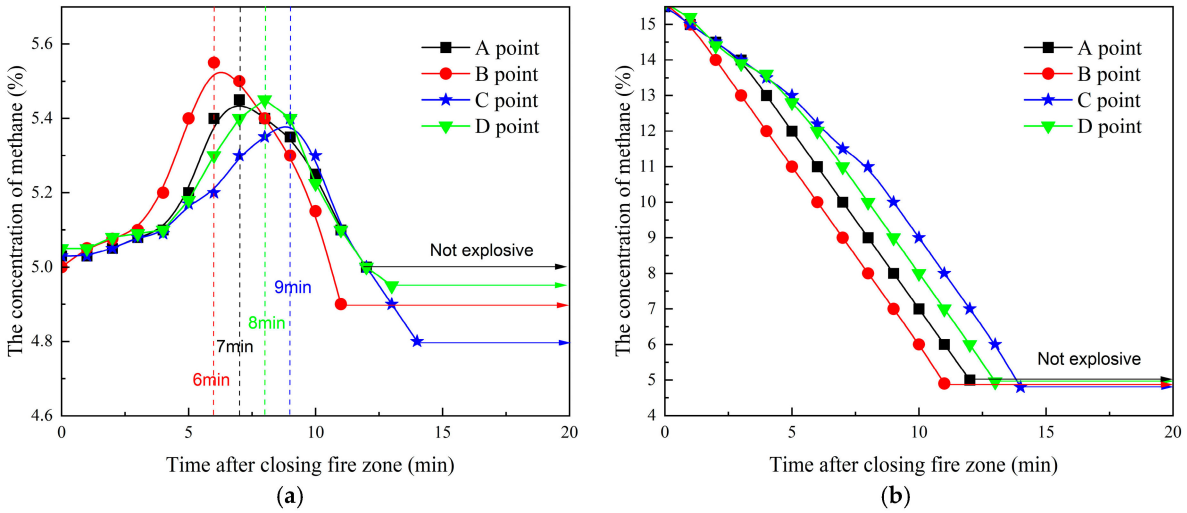

Figure 11. The variation of the minimum and maximum methane explosion for explosions in the fire zone. (**a**) The minimum methane concentration for explosions; (**b**) the maximum methane concentration for explosions.

The change in the minimum methane concentration for explosions after the closure of the fire zone is shown in Figure 11a. It can be seen that with the extension of closure time, the minimum methane concentration at each measuring point showed a trend of first increasing and then decreasing. The peak value appeared at four measurement points, A, B, C and D, after being closed for 7 min, 6 min, 9 min and 8 min, respectively. This was because in the initial stage of closure, coal combustion consumed a large amount of oxygen concentration, leading to a decrease in oxygen concentration near the fire zone, thereby causing an increase in the minimum methane concentration for explosions [23]. Among them, point B, which is closer to the fire zone, had the fastest decrease in O_2 concentration, resulting in the largest increase in the minimum methane concentration. Subsequently, as the combustion in the fire zone continued, higher concentrations of CO and C_2H_4 gas were generated, leading to a gradual decrease in the minimum methane concentration. However, when the closure time of the fire zone reached 10–15 min, the mixed combustible gases in the environment lose their explosiveness due to the O_2 concentration in the reaction system being lower than the critical oxygen concentration required for gas explosion [24]. The change in the maximum methane concentration for explosions after the closure of the fire zone is shown in Figure 11b. It can be seen that after the fire zone was closed, the maximum methane concentration for explosions at each measuring point showed a rapid downward trend. This was mainly attributed to the decrease in oxygen concentration in the fire zone environment and the generation of combustible gases, which together led to a decrease in the maximum methane concentration for explosions. Additionally, when the fire zone was closed for more than 15 min, the mixed combustible gases in the environment lost their explosiveness, which was consistent with the test results for the minimum methane concentration.

4. Conclusions

In the study, a three-dimensional physical model of gob was built, and the dynamics of CO and C_2H_4 distribution were delineated during the thermal escalation of coal under conditions of spontaneous combustion. Further, the explosion limits of methane enriched with CO and C_2H_4 mixtures were tested. The main conclusions of this paper are as follows:

- A three-dimensional physical test model of the gob was constructed according to the characteristics of the coal gob on a scale of 1:100, and the experimental platform mainly consisted of the air intake and return roadways, the working face, the gob, the temperature monitoring system, the ventilation system, the coal spontaneous combustion fire zone and the collection system.
- With the increase in coal temperature, CO and C_2H_4 mainly spread to the depth of the mining zone and the vicinity of the air return side. After sealing the fire zone, CO and C_2H_4 first formed a small-scale accumulation phenomenon near the fire zone. With the lowering of the temperature, the C_2H_4 and CO concentration dispersed towards the interior of the gob, but a small scale of C_2H_4 and CO still accumulated on the side of the return air corner.
- After the fire zone was sealed, the minimum methane concentration for explosions near the fire zone showed a trend of first increasing and then decreasing, while the maximum methane concentration for explosions decreased significantly. When the fire zone was closed for more than 15 min, the mixed combustible gases in the environment lost their explosiveness.

Author Contributions: D.M.: methodology, software, investigation, validation, visualization, data curation, writing—original draft. L.Z.: supervision, conceptualization, resources, writing—review and editing, project administration. T.Z.: supervision, resources. Z.S.: software, review and editing. All authors have read and agreed to the published version of the manuscript.

Funding: This work was supported by the Engineering Technology Research Centre for Safe and Efficient Coal Mining (Anhui University of Science and Technology) (NO. SECM2208) and the National Natural Science Foundation of China (NO. 52204250).

Institutional Review Board Statement: Not applicable.

Informed Consent Statement: Informed consent was obtained from all subjects involved in the study.

Data Availability Statement: The data are not publicly available due to commercial confidentiality, as they contain information that could compromise the privacy of research participants.

Conflicts of Interest: The authors declare no conflicts of interest.

References

1. Song, Z.; Kuenzer, C. Coal fires in China over the last decade: A comprehensive review. *Int. J. Coal Geol.* **2014**, *133*, 72–99. [CrossRef]
2. Ling, Y.; Luo, H. Current situation and development trend for coal mine fire prevention and extinguishing techniques in China. *Mei T'an Hsueh Pao (J. China Coal Soc.)* **2008**, *33*, 126–130.
3. Singh, R.V.K. Spontaneous heating and fire in coal mines. *Procedia Eng.* **2013**, *62*, 78–90. [CrossRef]
4. Geng, J.; Sun, Q.; Zhang, Y.; Gong, W.; Du, S. Non-destructive testing and temperature distribution of coal mine roadway lining structure under exogenous fire. *J. Loss Prev. Process Ind.* **2018**, *55*, 144–151. [CrossRef]
5. Zhou, F.B.; Li, J.H.; He, S.; Liu, Y.S. Experimental modeling study on the reignition phenomenon when opening a sealed fire zone. *Procedia Earth Planet. Sci.* **2009**, *1*, 161–168. [CrossRef]
6. Shi, G.Q.; Wang, G.Q.; Ding, P.X.; Wang, Y.M. Model and simulation analysis of fire development and gas flowing influenced by fire zone sealing in coal mine. *Process Saf. Environ. Prot.* **2021**, *149*, 631–642. [CrossRef]
7. Zuo, Q.; Li, J. Simulation of fire smoke disaster in a goaf during the closure process. *Therm. Sci.* **2021**, *25 Pt A*, 3399–3407. [CrossRef]
8. Zhu, C.G.; Wang, J.; Xie, W.X.; Zheng, T.T.; Lv, C. Improving strontium nitrate-based extinguishing aerosol by magnesium powder. *Fire Technol.* **2015**, *51*, 97–107. [CrossRef]
9. Taraba, B.; Pavelek, Z. Investigation of the spontaneous combustion susceptibility of coal using the pulse flow calorimetric method: 25 years of experience. *Fuel* **2014**, *125*, 101–105. [CrossRef]
10. Ma, T.; Larrañaga, M. Theoretical flammability diagram for analyzing mine gases. *Fire Technol.* **2015**, *51*, 271–286. [CrossRef]
11. Zhu, Y.; Wang, D.; Shao, Z.; Xu, C.; Zhu, X.; Qi, X.; Liu, F. A statistical analysis of coalmine fires and explosions in China. *Process Saf. Environ. Prot.* **2019**, *121*, 357–366. [CrossRef]
12. Duzgun, H.S.; Yaylaci, E.D. An evaluation of Soma underground coal mine disaster with respect to risk acceptance and risk perception. In Proceedings of the 3rd International Symposium on Mine Safety Science and Engineering, Montreal, QC, Canada, 13–19 August 2016; pp. 368–374.
13. Liang, Y.; Zhang, J.; Wang, L.; Luo, H.; Ren, T. Forecasting spontaneous combustion of coal in underground coal mines by index gases: A review. *J. Loss Prev. Process Ind.* **2019**, *57*, 208–222. [CrossRef]
14. Zhu, Y.; Zhou, X.; Wang, H.; Wang, B. *Numerical Simulation on Migrating Laws of Mixed Gas after Nitrogen Injection in Sealing Fire Zone of Coal Mine*; Coal Industry Publ House: Fuxin, China, 2008.
15. Wang, G.-Q.; Shi, G.-Q.; Wang, Y.-M.; Shen, H.-Y. Numerical study on the evolution of methane explosion regions in the process of coal mine fire zone sealing. *Fuel* **2021**, *289*, 119744. [CrossRef]
16. Brune, J.F.; Saki, S.A. Prevention of gob ignitions and explosions in longwall mining using dynamic seals. *Int. J. Min. Sci. Technol.* **2017**, *27*, 999–1003. [CrossRef]
17. Wen, H.; Guo, J.; Jin, Y.; Wang, K.; Zhang, Y.; Zheng, X. Experimental study on t influence of different oxygen concentrations on coal spontaneous combustion characteristic parameters. *Int. J. Oil Gas Coal Technol.* **2017**, *16*, 187–202. [CrossRef]
18. Zheng, Y.; Li, Q.; Zhang, G.; Zhao, Y.; Zhu, P.; Ma, X.; Li, X. Study on the coupling evolution of air and temperature field in coal mine goafs based on the similarity simulation experiments. *Fuel* **2021**, *283*, 118905. [CrossRef]
19. Wang, G.; Shi, G.; Yang, Y.; Liu, S. Experimental study on the exogenous fire evolution and flue gas migration during the fire zone sealing period of the coal mining face. *Fuel* **2022**, *320*, 123879. [CrossRef]
20. Li, L.; Qin, B.; Ma, D.; Zhuo, H.; Liang, H.; Gao, A. Unique spatial methane distribution caused by spontaneous coal combustion in coal mine goafs: An experimental study. *Process Saf. Environ. Prot.* **2018**, *116*, 199–207. [CrossRef]
21. Ma, D.; Qin, B.; Zhong, X.; Sheng, P.; Yin, C. Effect of flammable gases produced from spontaneous smoldering combustion of coal on methane explosion in coal mines. *Energy* **2023**, *169*, 128125. [CrossRef]
22. *BS EN 1839:2012*; Determination of Explosion Limits of Gases and Vapours. European Committee for Standardisation, BIS Standards Publication: Brussels, Belgium, 2012; p. 7.

23. Luo, Z.; Su, B.; Wang, T.; Cheng, F.; Wang, Y.; Liu, B.; Xie, C. Effects of propane on the flammability limits and chemical kinetics of methane–air explosions. *Combust. Sci. Technol.* **2020**, *192*, 1785–1801. [CrossRef]
24. Su, B.; Luo, Z.; Wang, T.; Zhang, J.; Cheng, F. Experimental and principal component analysis studies on minimum oxygen concentration of methane explosion. *Int. J. Hydrogen Energy* **2020**, *45*, 12225–12235. [CrossRef]